Synthesis and optical properties of white-light-emitting alumina/ZnO nanotubes

2008 Nanotechnology 19 405608

(http://iopscience.iop.org/0957-4484/19/40/405608)

Nanotechnology **19** (2008) 405608 (8pp) doi:10.1088/0957-4484/19/40/405608

Synthesis and optical properties of white-light-emitting alumina/ZnO nanotubes

Chi-Sheng Hsiao[1], San-Yuan Chen[1], Wan-Lin Kuo[1], Chin-Ching Lin[2] and Syh-Yuh Cheng[2]

[1] Department of Materials Sciences and Engineering, National Chiao Tung University, Hsinchu, Taiwan
[2] Materials Research Laboratories, Industrial Technology Research Institution, Chutung, Taiwan

E-mail: sanyuanchen@mail.nctu.edu.tw

Received 25 June 2008, in final form 20 July 2008
Published 21 August 2008
Online at stacks.iop.org/Nano/19/405608

Abstract

A simple chemical solution process was used to prepare alumina nanoparticle-coated ZnO nanotubes (ANZTs). Transmission electron microscope (TEM) images proved that the alumina nanoparticles were uniformly dispersed on the ZnO nanotubes. After thermal treatment at different temperatures under various atmospheres, photoluminescence (PL) measurements showed that the ANZTs emitted a variety of colors, including blue, green and white light. Gaussian curve fitting of the PL spectra revealed that the competition between the blue, blue-green, green and yellow band emissions and their relative emission intensities were strongly associated with various defects. Blue emission was attributed to large numbers of oxygen defects in alumina, while green and yellow emissions were related to oxygen and zinc defects in ZnO, respectively. Under specific conditions, white light, consisting of blue, blue-green, green and yellow band emissions, was obtained. Further TEM analysis indicated that the defect structure of ANZTs could be manipulated by the interface interaction between alumina and the ZnO nanotubes.

(Some figures in this article are in colour only in the electronic version)

1. Introduction

Zinc oxides (ZnO) have attracted extensive attention for nanoscale electronic and optoelectronic device applications because of their wide band gap and large excitation binding energy (60 meV) [1]. Numerous ZnO nanostructures have been demonstrated, including nanowires, nanotubes, and nanobelts [2–4]. It is believed that tubular structures exhibit higher porosity and larger surface area than bulk materials, creating enhanced performance and activity [5]. Recently, ZnO nanotubes have been fabricated by many methods, such as a hydrothermal process, a template-assisted method and a thermal oxidation process [6–8]. Almost all reports of ZnO nanotubes focus on morphologies, synthetic methods, and growth mechanisms. As mentioned above, however, the increased surface area is a key feature of tubular ZnO. Inevitably, high surface areas will significantly modify the chemical and physical properties of materials, which can be reflected in photoluminescence (PL) spectra.

Liu *et al* studied the optical properties of faceted hexagonal ZnO nanotubes (ZTs) and reported that a strong yellow emission was detected after annealing at 400 °C in ambient oxygen [9]. In contrast, Sun *et al* reported that after annealing at 400 °C for 2 h under vacuum, the PL spectrum of ZTs showed an increase in UV emission intensity and a concomitant decrease in green-yellow emission [10]. Zhang *et al* recently mentioned that a strong green emission was obtained from ZnO nanotubes annealed in H_2 [11]. Considering the large surface area-to-volume ratio in nanostructures, large numbers of defects and impurities at the surface of ZnO nanotubes can produce new states that act as visible luminescence centers and broaden

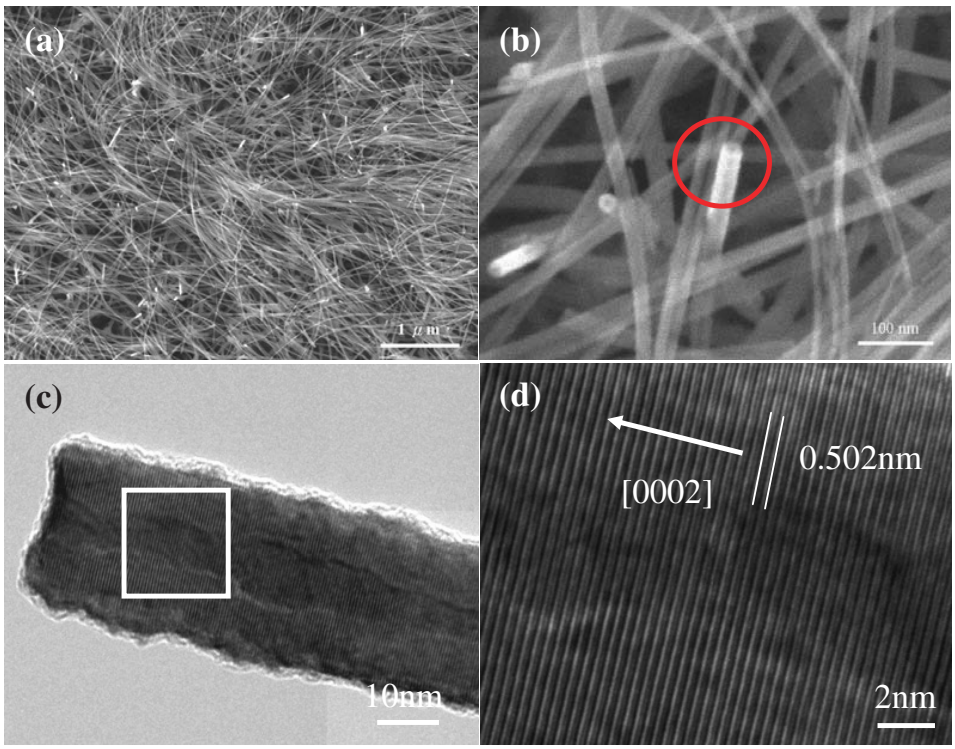

Figure 1. (a) SEM images of ZnO nanotubes. (b) High-magnification SEM image of ZnO nanotubes. (c) TEM images of a single ZnO nanotube. (d) High-resolution TEM image of a single ZnO nanotube.

the visible emission band. This suggests that the ZnO nanostructure could, after low-temperature growth and high-temperature annealing treatments, be developed for application in photoluminescent devices. In our previous study, we found that when an alumina film was deposited on ZnO nanorods and then annealed at 600 °C in a nitrogen ambient, the alumina-coated ZnO nanorods displayed a strong blue-light emission (the relative intensity (blue/UV) of the samples is up to 20) [12]. This indicated that ZnO strongly affected the photoluminescent properties of nanosized alumina films, leading to different UV to blue light intensity ratios in the PL spectra. Furthermore, depending on the processing methods, a variety of defects can be easily generated in nanostructured ZnO. Therefore, it is possible to develop white-light-emitting alumina-coated ZnO nanotubes if relative intensities of various color emission can be properly controlled by incorporating alumina into the ZnO nanostructure to modify the defects in ZnO nanotubes. To the best of our knowledge, there have been no other systematic investigations of the light-emitting properties of alumina-coated ZnO nanotubes synthesized at low temperatures.

In this work, we propose a simple method of combining the chemical process with thermal treatment to develop alumina-coated ZTs. In addition, we discuss the structure and photoluminescent properties of the alumina-coated ZTs. It has been demonstrated that the color of the emitted light can be varied with annealing processes at different temperatures and under different atmospheric conditions. White-light-emitting alumina-coated ZTs may be useful in novel nanoscale electric and optoelectronic devices.

2. Experimental details

Zinc nitrate hexahydrate ($Zn(NO_3)_2{\cdot}6H_2O$) was used as a zinc precursor to synthesize ZTs. Hexamethylenetetramine (HMT) was used to simultaneously precipitate the divalent post-transition metal Zn^{2+} ions [13]. An equimolar (0.001 M) aqueous solution of $Zn(NO_3)_2{\cdot}6H_2O$ and HMT was prepared. Subsequently, the substrates (ZnO_f/Si) were placed inside the solution at 95 °C for 24 h. The substrates were removed from the aqueous solutions, rinsed with distilled water and dried at 60 °C. To produce alumina nanoparticles, ammonia was added to an aqueous alumina nitrate solution (0.4 M) held at pH $\sim$ 10 at room temperature. After the hydrated precipitate was formed, it was centrifugally separated and washed several times with distilled water. The precipitate was dried in an oven at 120 °C for 6 h. Next, the precipitate was dispersed in the water solution by ultra-sonication and adjusted to pH 8.0 with ammonia. The precipitate with pseudo-boehmite phase (γ-AlO(OH)) will absorb OH^- ions to form –OO–Al–OH_2^+ on the surface. Then, the ZnO nanotubes will react with –OO–Al–OH_2^+ precursor to deposit alumina nanoparticles on the ZnO nanotubes after being immersed into the solution at 120 °C for 1 h [13]. After washing the alumina-coated ZTs with distilled water, rapid thermal annealing (RTA) was performed at 200–800 °C for 20 min under oxygen and nitrogen atmospheres. The samples were analyzed with a transmission electron microscope (TEM, JEOL 2100) operated at 200 keV. Room-temperature PL measurements were performed with a 325 nm He–Cd laser with an excitation power of 25 mW. The emitted luminescence

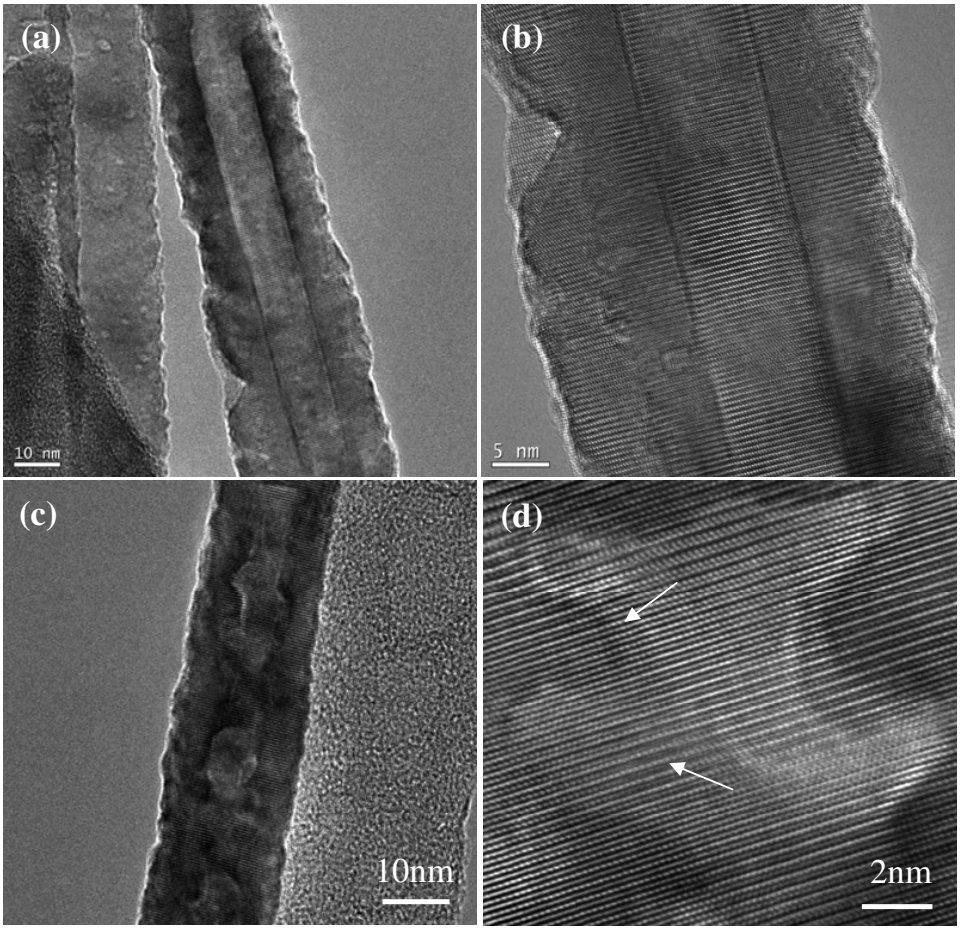

Figure 2. TEM images of Al_2O_3/ZnO nanocables annealed in oxygen at 400 °C at (a) low magnification and (b) high magnification and at 600 °C.

was detected with a 0.32 m spectrometer with a charge-coupled device detector. The focused spot size of the He–Cd laser was estimated to be about 200 μm in diameter.

3. Results and discussion

Figure 1 shows an SEM image of as-grown ZnO nanotubes synthesized in solution at 95 °C for 24 h. The low-magnification SEM image in figure 1(a) reveals that the nanotubes are several (2–5 μm) micrometers in length. The corresponding high-magnification SEM image in figure 1(b) shows that each nanotube has a uniform width over its entire length. The typical diameter is in the range of 20–30 nm. High-resolution transmission electron microscopy (figure 1(c)) shows that the ZTs are open-headed tubular structures with wall thicknesses of about 5–7 nm and inner diameters of about 15–20 nm. Figure 1(d), an enlargement of the marked area in figure 1(c), shows the highly preferential growth of ZnO nanotubes along the *c*-axis orientation (0002) with a lattice constant of ∼0.52 nm. Compared to ZnO nanowires, the disappearance of the *c*-axis plane of the ZnO nanotubes was clearly observed. In addition, rough inner surfaces were observed. Sun and co-workers reported that, during the formation of ZnO nanotubes in the solution, the concentration of all zinc-containing species falls and the concentration of OH^- increases with increasing t, leading to a progressive reduction in the overall zinc/OH^- ratio [14]. At first, the solution supersaturation falls below that required for growth. It may even fall to the point of triggering dissolution, as suggested by the appearance of volcano-like surface structures that serve as templates for the emerging nanotubes. With increasing time, the *c*-axis plane dissolves into $Zn(OH)_2$, forming the nanotube structure. Here, a rough inner surface was developed during the disappearance of the *c*-axis plane.

The ZTs were annealed in O_2 from 200 to 600 °C. At 200 °C, no obvious changes were observed in the SEM and TEM images. Figure 2(a) shows that ZTs annealed at 400 °C in ambient oxygen had a diameter of 30 nm. After annealing at 400 °C in oxygen ambient, the surface roughness increased on the outside surface probably due to the thermal etching seen in the TEM images in figure 2(a). Therefore, under these conditions, the diameter and wall thickness of the ZTs were possibly altered, and many surface defects were produced on the outside surface. The disappearance of the *c*-axis plane led to the formation of the nanotube structure, creating a rough inner wall at the initial stages. However, the inner surface morphology became flattened, as shown in figure 2(b). When the ZTs were thermally annealed, the atoms may possibly have obtained enough energy to rearrange into their native

morphology. To reduce the surface energy, the side plane wanted to flatten, but it was heavily thermally etched. It is believed that this is why the diameter of the ZTs decreased with increasing annealing temperature. When the annealing temperature increased to 600 °C, the low-magnification TEM image analysis of the ZTs indicated that the inner wall became very rough (figure 2(c)). Further investigation by high-resolution TEM analysis (figure 2(d)) demonstrated that the inner wall became wave-like in shape. The lattice fringe of the ZT was different (marked with two arrows), indicating that the wave shape was probably related to structure relaxation during the high-temperature treatment.

Figure 3 shows the room-temperature photoluminescence (PL) of ZTs annealed at different temperatures in oxygen ambient. Two obvious emission bands were observed: UV emission related to free exciton recombination at around 378 nm and broadband visible emission related to the oxygen defects. When the ZTs were annealed at 400 °C in oxygen, the outside surface was gradually thermally etched and became very rough, indicating that more surface defects were created. Under these conditions, the oxygen gas was easily absorbed on the ZT surface, producing more oxygen interstitials (O_i). This was especially true for hollow ZTs, which have a much higher surface/volume ratio than ZnO nanowires. Wu *et al* reported that oxygen interstitials may be the source of yellow emission [15]. Therefore, the yellow emission strengthened due to the increase of the oxygen defects and the UV emission intensified because increased annealing temperature decreased the number of structural defects.

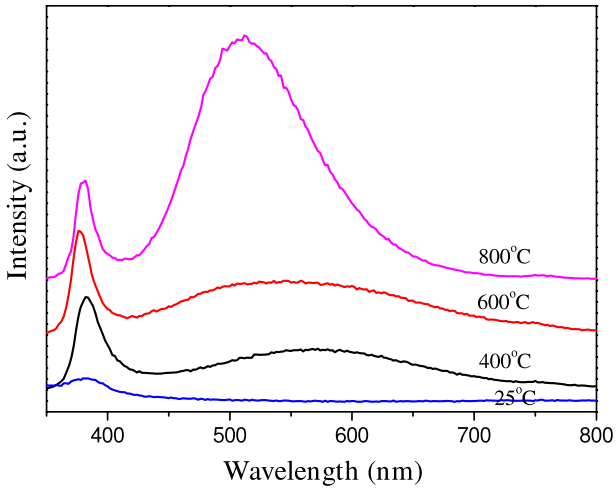

Figure 3. (a) Room-temperature PL spectra of ZnO nanotubes after rapid thermal annealing at various temperatures in O_2 atmosphere.

Increasing the annealing temperatures to 600 °C thermally etched both the outside and the inside surfaces of ZTs. The wave-like surface was confirmed by HRTEM analysis

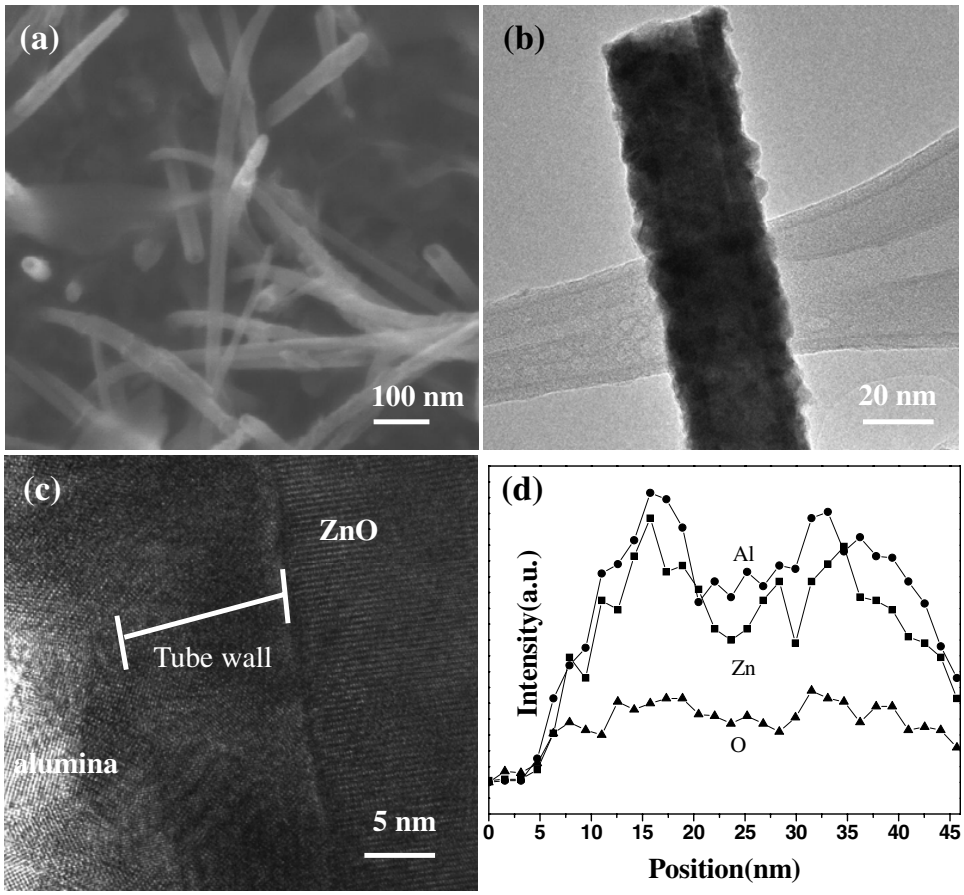

Figure 4. (a) SEM and (b) TEM images of the alumina nanoparticle-coated ZnO nanotubes. (c) High-magnification TEM images of the samples. (d) Intensity profile of Al, Zn, and O across and along one tube diameter.

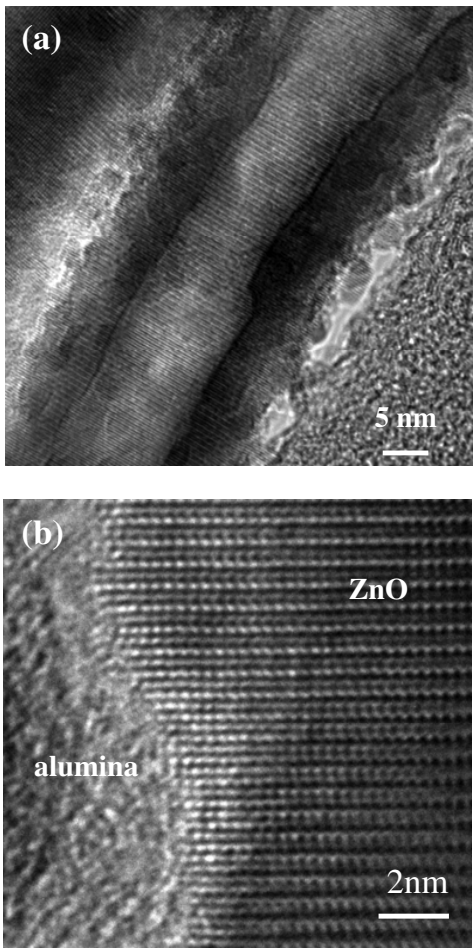

Figure 5. (a) High-magnification TEM images of (a) the interface and (b) the core of a sample annealed at 400 °C in ambient oxygen.

(figure 2(b)), indicating an increased surface-to-volume ratio with very high-temperature treatments. Therefore, the crystallinity of ZTs decreased as the UV emission decreased in the PL spectra. When the samples were annealed at high temperatures, antisite oxide O_{Zn} formed from interstitial oxygen O_i and zinc vacancies V_{Zn} in O-rich conditions [16, 17]. Therefore, the broadband visible emission resulted from O_i, V_{Zn} and O_{Zn} defects. It has been reported that at 800 °C antisite oxide forms, becoming the predominant source of point defects. In addition, the number of V_{Zn} defects increases. In our experiments, strong emission at 512 nm from O_{Zn} and V_{Zn} was observed.

Figure 4(a) shows an SEM image of ZnO nanotubes coated with a nanoparticle alumina shell by the solution process. The low-magnification TEM image in figure 4(b) proves that the ZTs were covered with a number of alumina nanoparticles. The diameters of the ZTs were about 40 nm. The corresponding high-magnification TEM image in figure 4(c) clearly shows that the alumina nanoparticles were crystalline and distributed well on the ZTs. EDX line-scanning analysis further confirmed that alumina had successfully coated the surface of the ZTs (figure 4(d)). When the temperature was increased to 400 °C, the alumina nanoparticles were clearly observed on the surface of the ZTs (figure 5(a)) but it was predicted that a phase transformation would occur in the alumina nanoparticles. The as-deposited alumina pseudo-boehmite phase would transform into γ-alumina according to a literature report [18]. However, it was observed that some interaction occurred on the surface of ANZTs. It was noted in the HRTEM image in figure 5(b) that lattice disorder appeared at the ZnO/Al_2O_3 interface. The generated defects (V_{Zn}, V_O) strongly influenced the optical properties and will be discussed later. Upon raising the temperature to 600 °C, as shown in figure 6(a), an interaction layer formed between the outside alumina layer and the surface of ZnO nanotubes. In addition, according to the Kirkendall effect, Zn atoms diffused into the alumina layer and several voids were formed in the core of the tubes, as shown with arrows in figure 6(b). The reaction would be expressed by the following equations [19].

$$Al_2O_3 \xrightarrow{ZnO} 2Al_{Zn} + 3O_o + V''_{Zn} + 2h^{\bullet}$$

$$2ZnO \xrightarrow{Al_2O3} 2Zn_{Al} + 2O_o + V^{\bullet\bullet}_o + 2e'.$$

The corresponding diffraction pattern clearly revealed that the ANZT structure consisted of ZnO nanotubes grown with (002) planes and polycrystalline γ-phase alumina. Figure 6(a) also shows lattice distortion and a local interaction at the ZnO/Al_2O_3 interface because of nanoscale effects. The lattice fringe changed from 5.2 Å inside the ZnO(002) to about 4.6 Å at the interface of ZnO/Al_2O_3. This may be related to the formation of a spinel structure reported in the literature [20].

To observe emission at 600–700 nm, a 400 nm optical pass was used, resulting in the appearance of 410 nm emission. Figure 7 shows the PL spectra of the ANZTs under different annealing conditions. As annealed in oxygen ambient, it was found that the PL spectra of the ANZTs exhibit a very broad peak from 425 to 750 nm, as shown in figure 7(a). Furthermore, it was also observed that the PL spectra are also changed with annealing atmosphere. As seen in figure 7(b), ANZTs annealed in nitrogen at different temperatures displayed one strong blue and one weak green-yellow peak. The broad green-yellow peak dominated at low annealing temperatures (below 600 °C), and a strong blue emission peak at ~450 nm occurred at 600 °C. The blue emission was primarily due to singly ionized oxygen vacancies in alumina [21]. Large numbers of oxygen vacancies in the ANZT alumina nanoparticle shell were produced by annealing in nitrogen at high temperature. The above-mentioned results indicated that the PL spectra of the alumina-coated ZnO nanotubes (ANZTs) could emit different colors by varying the annealing conditions. Figure 7(c) illustrates this with blue, green and white emissions.

The PL spectra of the ANZTs annealed in oxygen at different temperatures were further analyzed by Gaussian curve fitting, as shown in figure 8. The curve fitting of the PL spectra revealed the competition between the UV, blue, blue-green, green and yellow band emissions associated with various defects. The fit using a four peaks schema can be used to compare the relative intensity of the PL emission at the different spectral bands and only for this purpose.

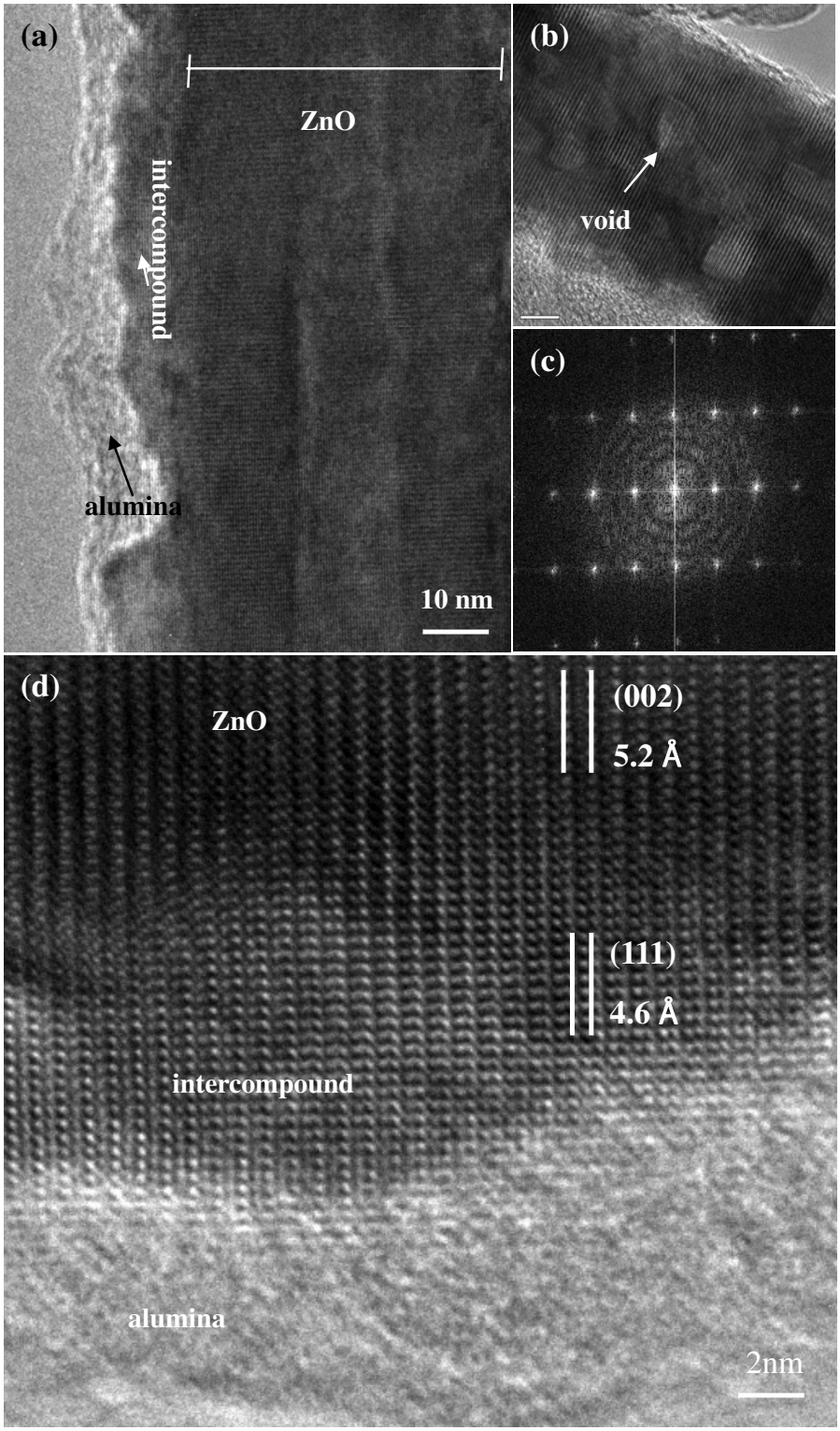

Figure 6. (a) TEM overview of samples. (b) Magnified mid-section images from samples annealed at 600 °C in oxygen. (c) The corresponding ED pattern. (d) High-resolution TEM images of interface of alumina and ZnO nanotubes.

Such a fit cannot describe the spectrum as a whole. When the samples were annealed at 200 °C in oxygen, the yellow emission dominated due to OH bond absorption on the surface of ANZTs. Increasing the annealing temperature to 400 °C increased the blue emission and decreased the yellow emission. The blue emission was probably related to phase transformation from the boehmite phase (octahedrally coordinated) to the γ-phase (tetrahedrally coordinated), which starts to appear at this temperature. During phase transformation, pentahedrally coordinated aluminum was produced, and singly ionized oxygen vacancies at the F^+ centers were responsible for the blue emission. For a detailed

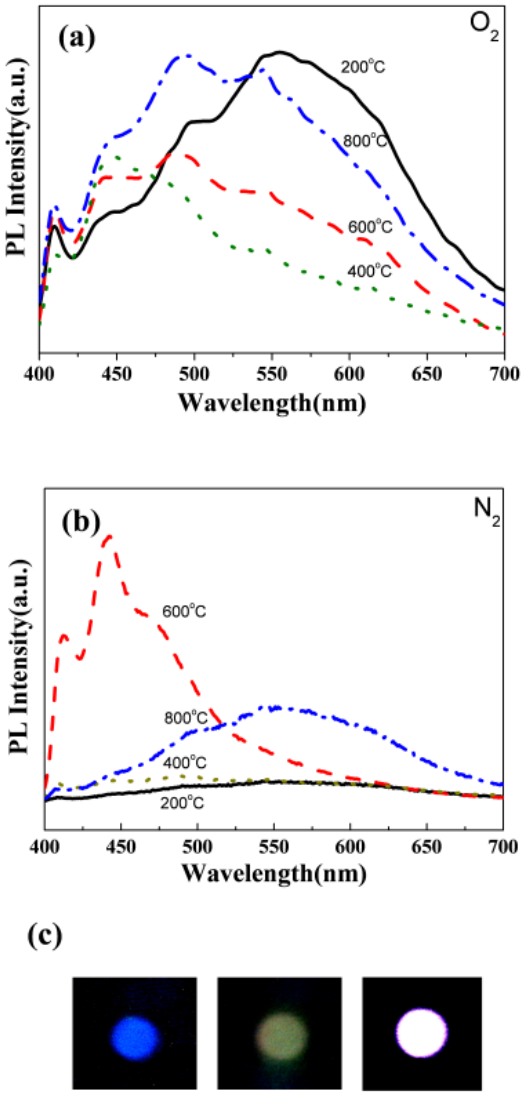

Figure 7. Room-temperature PL spectra of ZnO nanotubes after rapid thermal annealing at various temperatures in (a) O_2 and (b) N_2. (c) Blue, green and white photographs are shown in the left, middle and right of (c), respectively.

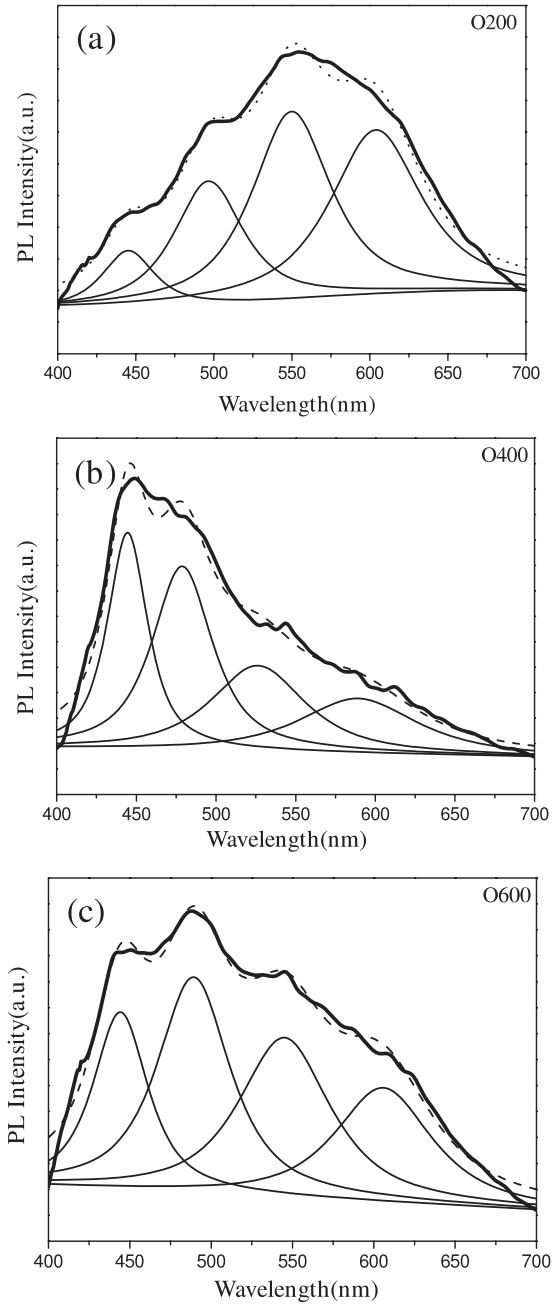

Figure 8. The Gaussian curve fit of PL spectra for samples annealed in oxygen at (a) 200 °C, (b) 400 °C, and (c) 600 °C.

discussion, refer to our previous study [12]. In general, the oxygen affinity in alumina is stronger than that in ZnO. Hence, the oxygen interstitials in the ZnO core diffused into the alumina shell, reducing the number of oxygen interstitials in ZnO. The number of oxygen vacancies in the ZT core nanotubes increased, leading to a strong green emission [22]. In addition, as shown in figure 5, an interaction occurred at the interface between the ZnO nanotube and the alumina layer. As the Zn atoms compounded with Al, the concentration of Zn atoms in the nanotubes decreased, and the concentration of V_{Zn} increased. Since the emission of V_{Zn} is located at ~496 nm, this created blue-green light. As a result, the relative intensity ratio of the four color peaks (blue:blue-green:green:yellow) was estimated to be 1.3:1.7:1.2:1 for the ANZTs annealed at 400 °C in oxygen.

Annealing ANZTs at a higher temperature (600 °C) compensated for the F^+ centers and reduced the blue emission. According to the report by Yang *et al*, the spinel structure might have been formed above 600 °C [23]. The HRTEM image marked with an arrow in figure 6(d) shows that an intercompound structure, possibly a spinel structure, composed of Zn and Al appeared in the interface between the ZnO nanotubes and the alumina layer. This made the blue-green emission peak strong. In addition, annealing increased the number of ZT surface defects and thus strengthened the yellow emission. At the same time, the green emission was also enhanced because the interaction on the interface induced a large number of oxygen vacancies in ZnO. Therefore, the relative intensity ratio of the four color peaks (blue:blue-green:green:yellow) changed to 0.86:1.23:1.11:1, leading to white emission.

4. Conclusion

In summary, we have developed alumina nanoparticle-coated ZnO nanotubes (ANZTs) on ZnO_f/Si substrates buffered with a ZnO film by combining simple chemical solution growth and annealing. The ANZTs emitted different light emissions as the annealing temperatures and atmospheres were changed. A white-light emission, consisting of blue, blue-green, green and yellow band emissions, was obtained. Photoluminescence measurements indicated a blue emission peak at ∼450 nm, a blue-green emission at ∼496 nm, a green emission peak at ∼525 nm, and a yellow emission peak at ∼600 nm. This work not only demonstrates a novel method for preparing white-light emission alumina-coated ZnO nanotubes, but also suggests that the defect structure and transition mechanisms of samples could be modified by different defect species.

Acknowledgments

The authors gratefully acknowledge the financial support of the National Science Council of the Republic of China and the Centre for Green Energy Technology, National Chiao Tung University through NSC96-2221-E-009-009 and 97W807, respectively.

References

[1] Laks D B 1993 *Appl. Phys. Lett.* **63** 1375
[2] Vayssieres L 2003 *Adv. Mater.* **15** 464
[3] Sun Y, Fuge G M, Fox N A, Riley D J and Ashfold M N R 2005 *Adv. Mater.* **17** 2477
[4] Kong X Y and Wang Z L 2003 *Nano Lett.* **3** 1625
[5] Chen C W, Chen K H C, Shen H, Ganguly A, Chen L C, Wu J J, Wen H I and Pong W F 2006 *Appl. Phys. Lett.* **88** 241905
[6] Vayssieres L, Keis K, Hagfeldt A and Lindquist S E 2001 *Chem. Mater.* **13** 4395
[7] Martinson A B F, Elam J W, Hupp J T and Pellin M J 2007 *Nano Lett.* **7** 2183
[8] Cheng J, Guo R and Wang Q M 2004 *Appl. Phys. Lett.* **85** 5140
[9] Tong Y, Liu Y, Shao C, Liu Y, Xu C, Zhang J, Lu Y, Shen D and Fan X J 2006 *J. Phys. Chem.* B **110** 14714
[10] Sun Y, Ndifor-Angwafor N G, Riley D J and Ashfold M N R 2006 *Chem. Phys. Lett.* **431** 352
[11] Zhang G, Adachi M, Ganjil S, Nakamura A, Temmyo J and Matsui Y 2007 *J. Appl. Phys.* **46** L730
[12] Hsiao C S, Kuo W L, Chen S Y, Shen J L, Lin C C and Cheng S Y 2008 *J. Electrochem. Soc.* **155** K96
[13] Barbara K H 2004 *Adv. Colloid Interface Sci.* **110** 19
[14] Sun Y, Riley D J and Ashfold M N R 2006 *J. Phys. Chem.* B **110** 15186
[15] Wu X L, Siu G G, Fu C L and Ong H C 2001 *Appl. Phys. Lett.* **78** 2285
[16] Wang J, Du G, Zhang Y, Zhao B, Yang X and Liu D 2004 *J. Cryst. Growth* **263** 269
[17] Quang L H, Chua S J, Loh K P and Fitzgerald E 2006 *J. Cryst. Growth* **287** 157
[18] Fitzgerald J J, Piedra G, Dec S F, Seger M and Maciel G E 1997 *J. Am. Chem. Soc.* **119** 7832
[19] Lin S S and Huang J L 2003 *J. Mater. Res.* **18** 965
[20] Fan H J, Knez M, Scholz R, Nielsch K, Pippel E, Hesse D, Zacharias M and Gosele U 2006 *Nat. Mater.* **5** 627
[21] Du Y, Cai W L, Mo C M, Chen J, Zhang L D and Zhu X G 1999 *Appl. Phys. Lett.* **74** 2951
[22] Lin C C, Liao H C and Chen S Y 2006 *J. Vac. Sci. Technol.* B **24** 304
[23] Yang Y, Kim D S, Knez M, Scholz R, Berger A, Pippel E, Hesse D, Gosele U and Zacharias M 2008 *J. Phys. Chem.* C **112** 4068